land

MDPI

Article

Distribution Patterns and Influencing Factors Controlling Soil Carbon in the Heihe River Source Basin, Northeast Qinghai–Tibet Plateau

Meiliang Zhao [1,2,*], Guangchao Cao [1,2,3,*], Qinglin Zhao [1,2], Yonggui Ma [3,4], Fuling Zhang [5], Hongda Li [6], Qixin He [1,2] and Xunxun Qiu [1,2]

1. Key Laboratory of Environmental Surface Processes and Ecological Conservation, Ministry of Education, Qinghai Normal University, Xining 810008, China; 2025036@qhnu.edu.cn (Q.Z.); 202247341004@stu.qhnu.edu.cn (Q.H.); 202247341007@stu.qhnu.edu.cn (X.Q.)
2. Key Laboratory of Physical Geography and Environmental Processes of Qinghai Province, College of Geography, Qinghai Normal University, Xining 810008, China
3. Qinghai Provincial Government—Beijing Normal University Institute of Plateau Science and Sustainable Development, Xining 810008, China; 2025041@qhnu.edu.cn
4. Academy of Life Science, Qinghai Normal University, Xining 810008, China
5. Provincial Natural Resources Remote Sensing Center of Qinghai Province, Xining 810008, China; linger0110@126.com
6. Qinghai General Station of Grassland, Xining 810008, China; lihongda1018@163.com

* Correspondence: zhaomeiliang2014@163.com (M.Z.); caoguangchao@qhnu.edu.cn (G.C.)

Abstract: Soil organic carbon (SOC) and soil inorganic carbon (SIC) are key components of soil carbon pools in arid ecosystems, playing a crucial role in regional carbon cycling and climate change mitigation. However, the interactions between these two forms of carbon in arid alpine ecosystems remain underexplored. This study was conducted in the Heihe River Basin (HRB) in the northeastern Qinghai–Tibet Plateau, focusing on the distribution and dynamics of SOC and SIC in deep soil layers. Using data from 329 samples collected from 49 soil profiles extending to the bedrock, combined with path analysis, we explored the inter-relationships between SOC and SIC and quantified the influence of environmental factors. The results showed that (1) SOC exhibited a unimodal distribution with elevation, peaking at 3300–3600 m, while SIC continuously decreased with elevation, with reduction rates ranging from −0.39% to −31.18%; (2) SOC and SIC were significantly positively correlated (r = 0.55, $p < 0.01$), with SOC decreasing with depth and SIC showing an inflection point at 50 cm depth; (3) SOC was primarily driven by nutrient factors, such as total nitrogen (TN), with a path coefficient of 0.988, while SIC was influenced by abiotic factors, including potential evapotranspiration (PET), with a coefficient of −1.987; (4) SOC density accounted for 81.62% of the total soil carbon pool, playing a dominant role in carbon storage, whereas SIC density exhibited dynamic changes, particularly at depths of 110–150 cm. These findings advance our understanding of deep soil carbon dynamics in arid alpine ecosystems and provide critical data for improving carbon management strategies in similar regions.

Keywords: soil organic carbon; soil inorganic carbon; path analysis; the Qinghai–Tibet Plateau

check for updates

Academic Editor: Nick B. Comerford

Received: 9 January 2025
Revised: 9 February 2025
Accepted: 13 February 2025
Published: 16 February 2025

Citation: Zhao, M.; Cao, G.; Zhao, Q.; Ma, Y.; Zhang, F.; Li, H.; He, Q.; Qiu, X. Distribution Patterns and Influencing Factors Controlling Soil Carbon in the Heihe River Source Basin, Northeast Qinghai–Tibet Plateau. *Land* **2025**, *14*, 409. https://doi.org/10.3390/land14020409

1. Introduction

Soil carbon reservoirs are fundamental to soil functionality and are critical in maintaining soil productivity and mitigating climate change [1,2]. According to statistical data, soil is the primary carbon repository within terrestrial ecosystems, harboring approximately 1500 Pg of soil organic carbon (SOC) and 700–1000 Pg of soil inorganic carbon (SIC) [3,4]. In China alone, an estimated 80–120 Pg of SOC and 53–78 Pg of SIC are sequestered [5,6]. Hence, even slight changes in atmospheric concentrations can precipitate substantial fluctuations, thereby exerting a substantial impact on the global climate [7]. With escalating global climate change and substantial alterations in ecological landscapes, the soil carbon pool has become a focal point in studies on terrestrial ecosystem carbon cycles and global transformations [8–10]. Furthermore, it is a core subject of numerous global research initiatives targeting environmental shifts, such as the Global Carbon Program and World Climate Research Program [11,12].

Soil carbon in arid regions constitutes approximately 52% of the global soil carbon pool [13,14], with 32% of the global SOC and 80% of the SIC situated therein [15]. Integral with the global carbon cycle, the carbon cycle in arid regions plays a crucial role in regional soil carbon pools, carbon budgets, and broader global biogeochemical cycles. Previously, SIC was believed to remain relatively stable over extended historical periods, thus exerting a limited influence on the carbon cycle of terrestrial ecosystems [16,17]. However, recent studies have highlighted rapid changes in the formation and turnover of secondary carbonates in response to climate warming, challenging the traditional perceptions of SIC [18]. Consequently, akin to SOC, SIC represents a significant carbon reservoir in ecosystems, although it has received less attention historically. Studies on the Mongolia Plateau [19] and Loess Plateau [20] in China show that SIC is the main component of soil carbon pools in arid areas. While some studies have suggested that SOC is a predominant component of the soil carbon pool in the hinterland of the Qinghai–Tibet Plateau (QTP) [21], our understanding of the changes in deep soil carbon in the QTP remains limited due to data constraints. The variation in soil carbon and the relationship between SOC and SIC in the QTP is not yet well understood.

Recent research emphasizes the need for a more integrated understanding of SOC and SIC, particularly in the context of climate change and land use. Both SOC and SIC play essential roles in the global carbon cycle, but their dynamics are shaped by different biotic and abiotic factors. SOC is primarily influenced by biological processes such as biomass input and litter decomposition, while SIC is governed by chemical and physical processes, including soil pH and moisture [22]. In arid and semi-arid regions, where SIC dominates, the relationship between these two carbon forms is particularly complex. Some studies have shown a positive correlation between SOC and SIC in agricultural lands [23], while others suggest an inverse relationship, especially in areas with high soil acidity or lower precipitation [21]. These findings highlight the importance of considering both SOC and SIC when studying soil carbon dynamics, as they contribute differently under varying environmental conditions. The Heihe River Basin (HRB), situated in the northeastern region of the QTP in the arid terrain of northwest China, serves as a transitional zone between the QTP and the Loess Plateau. Mi et al. [24] estimated that approximately 84% of SIC in China is stored in regions receiving less than 500 mm of annual precipitation. In the HRB, the annual precipitation ranges between 289.9 and 535.8 mm. Distinctive climatic conditions and geographical positioning make it an ideal location for investigating SOC and SIC dynamics in arid alpine ecosystems. The distribution and accumulation of SOC and SIC are fundamentally governed by soil-forming factors, including parent material, climate, organisms, topography, and time. For example, precipitation strongly influences carbonate leaching and accumulation, leading to the formation of calcic horizons [25]. This study builds upon these theoretical foundations to investigate SOC and SIC dynamics in the arid alpine ecosystem of the Heihe River Basin. The objectives of our study were twofold: (1) to analyze the distribution patterns of SOC and SIC in alpine arid ecosystems and their inter-relationships and (2) to investigate the influence of soil physicochemical properties and environmental factors on SOC and SIC, elucidating the primary influencing factors and pathways. These findings significantly enhance our understanding of deep soil carbon dynamics in arid alpine ecosystems and provide critical data and insight into similar regions.

2. Materials and Methods

2.1. Study Area

The HRB is situated in the hinterland of the Qilian Mountains, within the arid expanse of northwest China. It is the second-largest inland river in China, with a total length of 820 km, and plays a pivotal role in maintaining ecological security in the region [26]. The HRB (98°–101° E, 37.5°–39° N) constitutes the primary flow-generating area of the basin. This area exhibits significant topographical variations, with elevations ranging from 2256 m to 5281 m, encompassing an area of approximately 1.1×10^4 km^2 (Figure 1). Meteorological data from 1961 to 2019 reveal that annual precipitation in this region varies between 289.9 and 535.8 mm, while the average annual temperature is approximately −0.99 °C, indicative of an alpine arid continental climate. At elevations greater than 3400 m, permafrost is widely distributed throughout the HRB, making it a quintessential alpine mountain ecosystem in China [27].

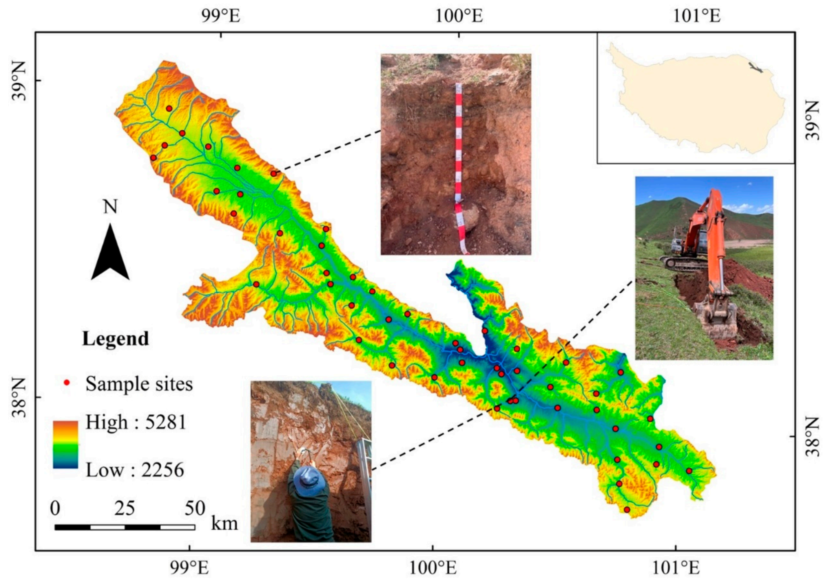

Figure 1. Distribution of sampling points in the Heihe River Basin.

2.2. Data Collection and Analysis

In July 2023, a comprehensive soil sampling campaign was conducted in the HRB, yielding a total of 49 representative soil profiles. The sampling strategy meticulously considered various factors, including land use type, vegetation cover, and elevation. Specifically, five profiles were collected from areas with elevations below 3000 m, 10 profiles from elevations between 3000 m and 3300 m, and 17 profiles from elevations between 3300 m and 3600 m. Moreover, 12 profiles were obtained from elevations between 3600 and 3900 m, and five profiles were obtained from elevations above 3900 m. To ensure a well-distributed representation across different elevations, the sampling points were strategically chosen, with the majority of profiles extending to depths greater than 90 cm. To facilitate a comprehensive analysis of the deep soil carbon characteristics, an excavator was employed to excavate a section approximately 230 cm deep at an altitude of 3167 m for additional sampling (Figure 1). All soil samples were meticulously collected at intervals of

10 cm within the top 30 cm layer and intervals of 20 cm below the 30 cm depth threshold. A total of 329 soil samples were collected. Undisturbed stratified soil samples were acquired using a 250 cm^3 European ring cutter for subsequent analysis of soil bulk density (BD). Soil water content (SWC) measurements were conducted using the gravimetric method, with samples dried to a constant weight in an oven at 105 °C, in accordance with the protocol outlined by Walter et al. [28]. Additionally, a handheld GPS device was used to determine the elevation and aspect of each sampling site, ensuring a comprehensive documentation of the sampling locations.

The collected soil samples were subjected to a series of analytical procedures for comprehensive characterization. First, the soil was air-dried, mixed, and sieved through a 2.0 mm sieve to determine pH and conductivity, following the method described by Dai et al. [29]. Subsequently, the composition of the soil particles was analyzed using a Mastersizer 2000 laser particle size analyzer (Malvern Panalytical, Malvern, UK) to determine the percentage of soil particles according to the US Soil Classification System. Total phosphorus (TP) and total potassium (TK) levels were quantified using the reagent method. Soil carbon and nitrogen contents were assessed using a Vario ISOTOPE cube elemental analyzer (Elementar, Langenselbold, Hesse, Germany). SIC was determined based on the difference between the total carbon and SOC. To facilitate the analysis, the sample data were further processed at intervals of 0–10, 10–30, and >30 cm. Meteorological and environmental data were obtained in August 2023 from the Resource and Environmental Sciences Data Center (https://www.resdc.cn, accessed on 12 February 2025). Soil carbon density was calculated according to the method described by Yang et al. [30]. A Pearson's correlation coefficient was used to assess the relationship between soil carbon and other relevant factors. Furthermore, the direct and indirect impacts of the major environmental factors were evaluated through a path analysis, following the approach described by Zhang et al. [31]. These analytical techniques and statistical methods were employed to comprehensively understand the dynamics and factors that influence soil carbon in the study area.

3. Results and Analyses

3.1. Distribution Pattern of SOC and SIC

Figure 2 illustrates the spatial distribution of the soil sampling points across the elevation gradient, accompanied by the corresponding average soil carbon content. SOC demonstrates an initial increase followed by a decrease with elevation, reaching its peak value (42.96 ± 4.86 g/kg) within the altitude range of 3300–3600 m and its lowest value (24.7 ± 7.37 g/kg) below the 3000 m elevation mark. This pattern likely reflects the combined effects of vegetation productivity, temperature, and organic matter decomposition. The altitude range of 3300–3600 m provides optimal conditions for vegetation growth and organic matter accumulation, leading to the peak in SOC. However, other ecological processes, such as changes in soil microbial community structure, could also contribute significantly to SOC accumulation in this elevation range. Soil microbes are essential for organic matter decomposition, and their activity is influenced by factors such as vegetation inputs and temperature. In this region, microbial activity likely supports greater carbon sequestration, contributing to the observed SOC peak. At altitudes below 3000 m, higher temperatures accelerate organic matter decomposition, which leads to a decrease in SOC. At altitudes above 3600 m, the decline in SOC may result from reduced vegetation cover, lower organic inputs, and harsher climatic conditions that limit microbial activity and organic matter accumulation. Conversely, SIC content exhibited a declining trend with increasing elevation, with the rate of decline accelerating as elevation increased (ranging from 0.39% to 31.18%). This suggests that SIC is more dominant in lower elevations where arid conditions and strong evaporation promote carbonate precipitation. At higher elevations, increased precipitation and lower temperatures favor the dissolution and leaching of carbonates, reducing SIC accumulation. These findings highlight the contrasting drivers of SOC and SIC distributions, with SOC being primarily controlled by biological factors, such as vegetation and organic inputs, while SIC is driven by abiotic processes, including soil hydrology, carbonate chemistry, and the dissolution–precipitation processes influenced by temperature and moisture.

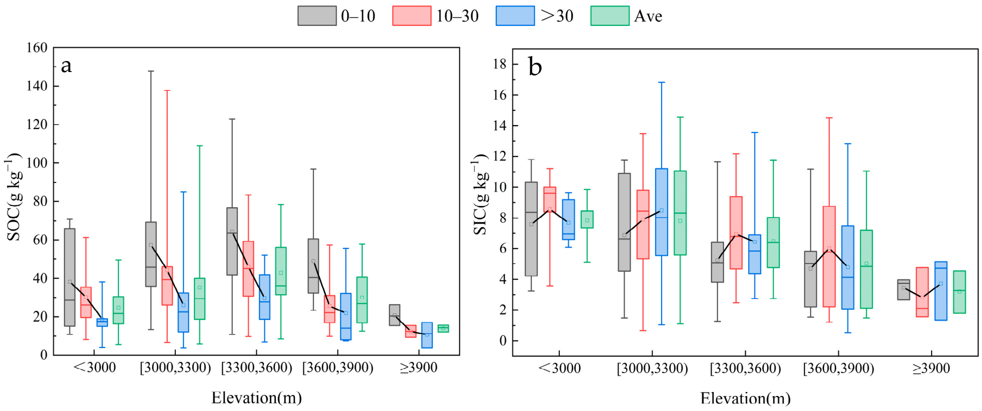

Figure 2. Distribution of soil carbon along the elevation gradient at the designated sampling points. ((**a**) Organic carbon distribution, (**b**) inorganic carbon distribution).

At various elevation gradients, SOC decreased with increasing soil depth. Below 3600 m, SOC exhibited a continuous decline in deeper soil layers, likely due to reduced organic inputs and microbial activity at depth. However, above 3600 m, SOC levels in the 10–30 cm and >30 cm soil layers showed no significant differences, indicating that SOC is predominantly concentrated in the surface or shallow soils within the alpine arid ecosystems. Conversely, SIC showed an initial increase and then a decrease with soil depth, typically peaking within the 10–30 cm soil layer. This pattern may reflect carbonate precipitation processes, which are influenced by soil hydrology and CO_2 concentration, with the 10–30 cm layer acting as a zone of carbonate accumulation. To corroborate these findings, we selected three representative sampling sites for a detailed analysis, taking into account factors such as elevation, vegetation, and soil (Figure 3). Figure 3 illustrates that SOC decreased with soil depth at all three sampling points, with the rate of decline gradually slowing. This pattern underscores the role of surface vegetation input and microbial activity in SOC distribution. Except for sampling site No. 717, SIC increased with soil depth up to 50 cm but decreased beyond that depth. At site No. 717, SIC exceeded SOC as a significant component of total soil carbon, particularly in deeper layers, likely due to enhanced carbonate accumulation under forest vegetation. In contrast, at sites No. 740 and No. 731, SIC was concentrated in the 10–30 cm layer, consistent with the broader elevation trends. Despite these variations, SOC remained the primary contributor to total soil carbon across most of the region (Figures 2 and 3).

Based on Table 1, there are significant differences in the organic carbon (SOC) and inorganic carbon (SIC) content at different soil depths (0–10 cm, 10–30 cm, >30 cm) between grassland and shrubland systems. At the 0–10 cm depth, the organic carbon content in grassland is 49.65 g kg^{-1}, while in shrubland it is 69.6 g kg^{-1}, indicating that shrubs contribute to a higher accumulation of organic carbon in the surface soil. As soil depth increases, the difference in organic carbon content between grassland and shrubland decreases. At the >30 cm depth, the difference becomes more pronounced (grassland 19.43 g kg^{-1}, shrubland 37.35 g kg^{-1}), showing that shrubland systems have an advantage in accumulating organic carbon in deeper soil layers. Regarding inorganic carbon, the differences between grassland and shrubland systems are relatively small. Overall, the trend shows that inorganic carbon content increases slightly with soil depth. In shrubland, inorganic carbon content is slightly higher than in grassland at all depths, but the difference is not significant. In summary, shrubland systems exhibit higher organic carbon accumulation both in surface and deeper soil layers, while inorganic carbon variation is more influenced by soil depth, with little difference between the two systems.

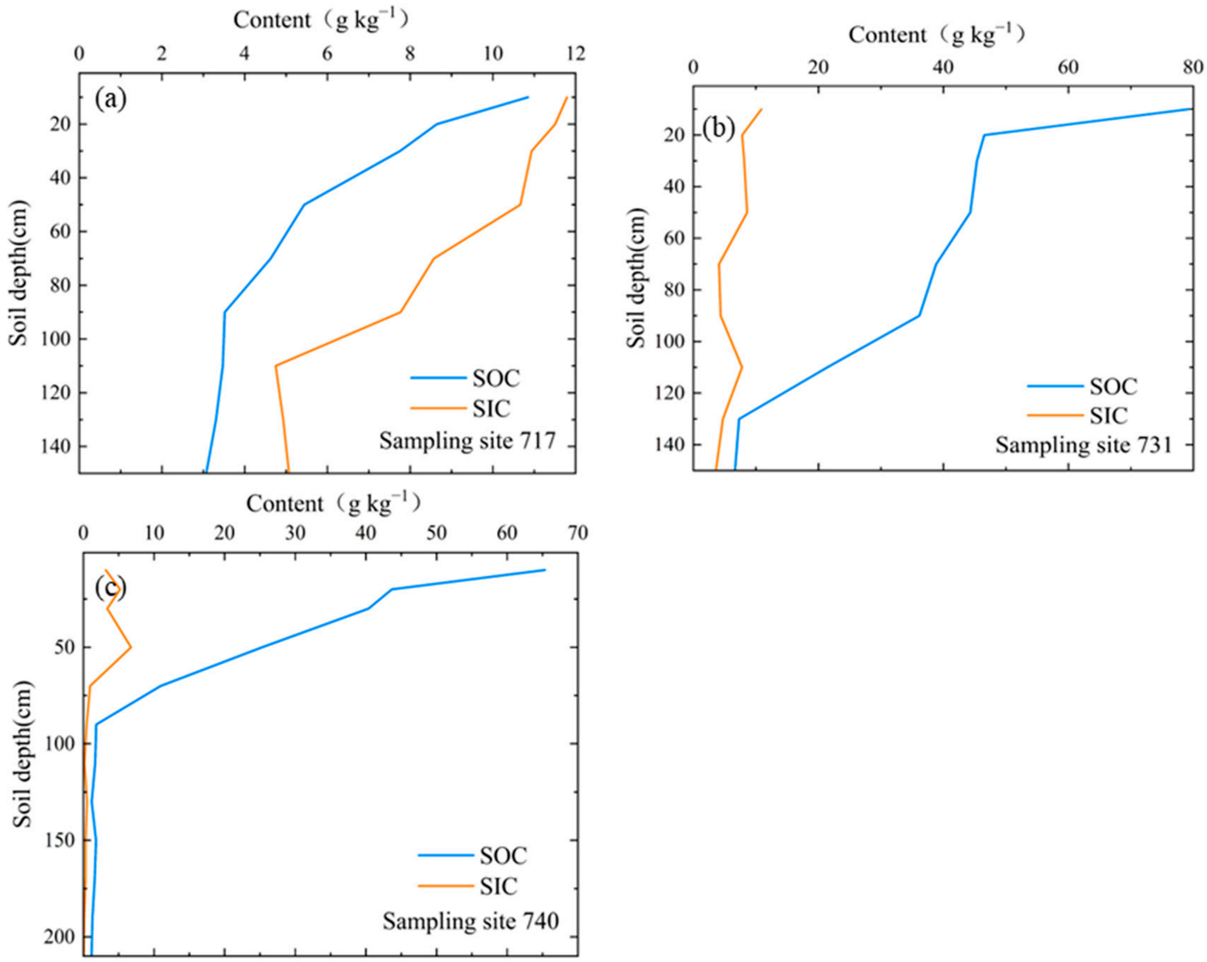

Figure 3. Vertical distribution of soil carbon at three representative sampling sites. SOC, soil organic carbon; SIC, soil inorganic carbon. ((**a**) 717 Sampling point, (**b**) 731 sampling point, (**c**) 740 sampling point).

Table 1. SOC and SIC changes under various LULC patterns.

Variable	Land Use/Land Cover	Soil Depth (cm)		
		0–10	10–30	>30
SOC (g kg^{-1})	Grassland	49.65	31.4	19.43
	Shrub	69.6	52.34	37.35
SIC (g kg^{-1})	Grassland	5.44	6.32	5.27
	Shrub	6.6	8.19	8.59

3.2. Distribution Pattern of Soil Organic Carbon Density and Soil Inorganic Carbon Density

Although SOC decreased with increasing soil depth, SIC exhibited an inflection point at 50 cm, indicating a shift in the dominant carbon forms within the soil profile. Our examination of soil carbon density revealed that SOCD was predominant in surface and shallow soils, reflecting higher organic matter inputs and microbial activity in these layers. Interestingly, in the 110–150 cm soil layer, SOCD accounted for 54% of the carbon pool, challenging the inorganic carbon dominance in deeper soils. Beyond 150 cm, SOCD regained its dominance, highlighting its importance as a persistent contributor across all depths (Table 2). Soil inorganic carbon density (SICD) demonstrated an initial increase, peaking at 50–70 cm, before decreasing with further depth. This pattern is likely shaped by carbonate precipitation, which is most active under optimal moisture and pH conditions in this layer. The inflection point of SICD, occurring one layer deeper than that of SIC, suggests a lag in carbonate redistribution compared to SOC cycling. Interestingly, the maximum values of both SOCD and SICD at 50–70 cm indicate potential interactions between organic and inorganic carbon processes.

Table 2. Changes in the vertical distribution of soil organic carbon density (SOCD) and soil inorganic carbon density (SICD).

Soil Depth (cm)	Changes in SOCD and SICD Proportion of Carbon Pool in the Same Soil Layer (%)		Vertical Distribution of SOCD and SICD (%)	
	SOCD	SICD	SOCD	SICD
0–10	89.01	10.99	11.53	4.60
10–20	84.39	15.61	9.25	5.53
20–30	81.72	18.28	9.29	6.72
30–50	79.16	20.84	17.57	14.95
50–70	76.97	23.03	18.80	18.18
70–90	71.10	28.90	13.48	17.71
90–110	74.34	25.66	12.94	14.43
110–130	54.35	45.65	3.39	9.21
130–150	54.65	45.35	3.15	8.44
150–170	83.28	16.72	0.21	0.14
170–190	90.03	9.97	0.21	0.08
190–210	95.03	4.97	0.17	0.03

As depicted in Figure 4, the spatial distribution of the soil carbon pool gradually diminished from southeast to northwest, with SOCD playing a predominant role in shaping this gradient. The southeast region, characterized by higher precipitation and vegetation cover, supports greater SOC inputs and accumulation, while the drier and less vegetated northwest restricts SOC storage. Regions with relatively high SICD values were primarily scattered across shallow mountain zones and away from river channels. These areas benefit from limited leaching and enhanced carbonate precipitation under drier conditions, contrasting with river-adjacent regions where stronger leaching likely reduces carbonate retention. However, due to the relatively smaller SICD values, their influence on the overall spatial distribution of the soil carbon pool remains minimal. The mean values of SOCD and SICD were 24.23 kg C m^{-2} and 5.46 kg C m^{-2}, respectively, indicating that SOCD accounted for 81.62% of the total soil carbon pool, serving as the primary carbon pool in the region. Despite its lower contribution, SICD plays a crucial role in deeper soil layers, particularly in the 110–150 cm range where SOCD and SICD exhibit near-equal significance. This layer represents a critical transition zone where interactions between organic and inorganic carbon pools may be most pronounced, influencing the long-term stability of the soil carbon pool.

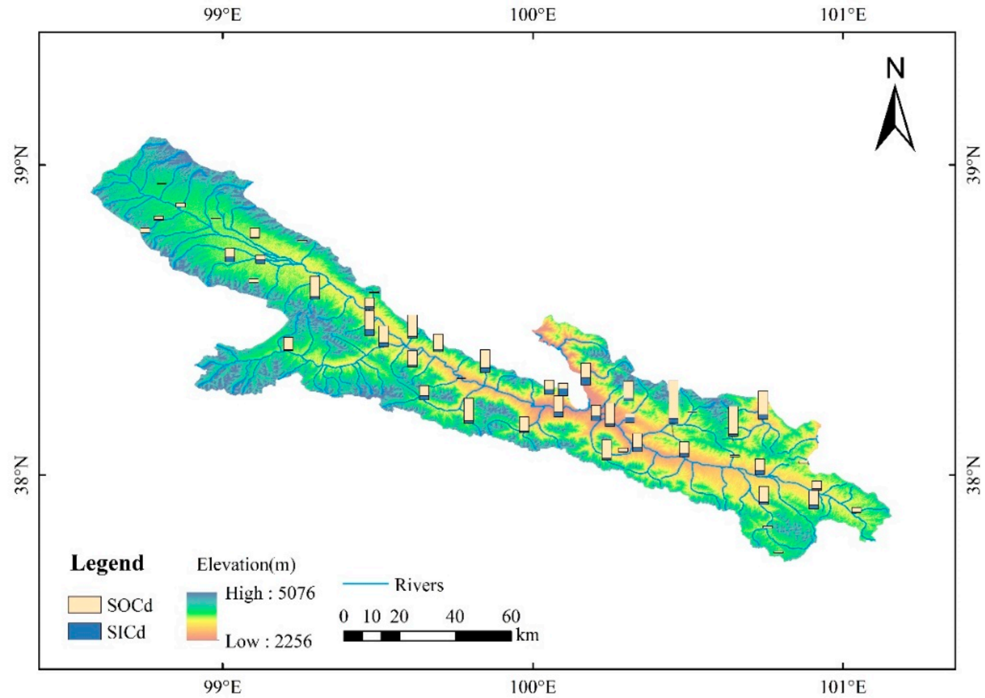

Figure 4. Spatial distribution pattern of soil organic carbon density (SOCD) and soil inorganic carbon density (SICD) based on sampling point scale.

3.3. Factor Analysis

3.3.1. Correlation Analysis

Figure 5 illustrates the relationship between soil carbon and various factors. The aspect (ASP), precipitation (PRE), NDVI, total nitrogen (TN), and silt content exhibited positive correlations with SOC and SIC, while sand content showed a negative correlation. These relationships highlight the importance of vegetation and soil texture in carbon storage. NDVI and PRE promote SOC accumulation through increased organic inputs, while silt content enhances SOC retention by protecting it within soil aggregates. Conversely, sandier soils, with lower nutrient and water retention, are less conducive to SOC and SIC accumulation. Soil depth (DEP), mean annual temperature (TEM), and potential evapotranspiration (PET) negatively impacted SOC, reflecting the reduced organic inputs and accelerated decomposition in deeper, warmer, and drier soils. In contrast, the aridity index (AI) promoted SOC, likely due to reduced microbial decomposition under drier conditions, while inhibiting SIC formation, as insufficient moisture limits carbonate precipitation. Soil water content (SWC) showed contrasting effects on SOC and SIC. High SWC supported SOC accumulation by enhancing vegetation growth and slowing decomposition while inhibiting SIC by promoting carbonate dissolution and leaching. Similarly, soil pH was negatively correlated with SOC but positively correlated with SIC, indicating that acidic conditions stabilize SOC while alkaline conditions favor carbonate formation. In summary, SOC is primarily driven by vegetation, soil texture, and moisture, while SIC is more influenced by soil pH and aridity. These findings highlight the complementary roles of SOC and SIC in the carbon cycle and the need for further exploration of their interactions under changing environmental conditions.

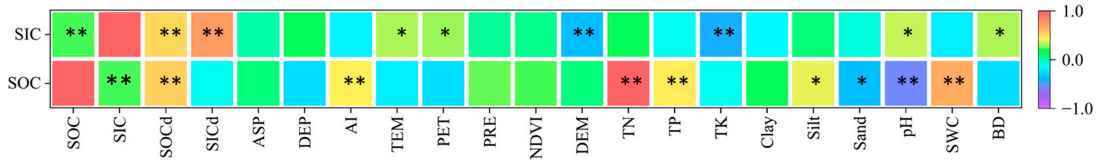

Figure 5. Correlation between soil carbon and other elements. Note: ** denotes significance at $p < 0.01$ and * denotes significance at $p < 0.05$.

3.3.2. Path Analysis

We employed a path analysis, based on a correlation analysis and a stepwise multiple linear regression equation, to dissect the direct and indirect effects of environmental factors on SOC and SIC. This statistical method enabled us to quantify the relative influence of variables such as TN, SWC, and elevation, providing a comprehensive understanding of the causal relationships driving soil carbon dynamics (Figure 6).

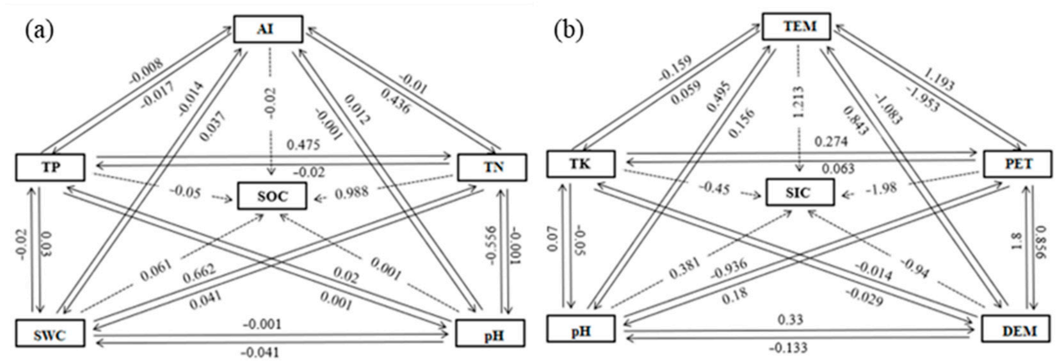

Figure 6. Path coefficient diagram between soil carbon content and other influencing factors. Dashed arrows represent the direct effects of the respective factors on soil carbon content, whereas solid arrows represent the indirect effects of the respective factors on soil carbon content, mediated by another factor. ((**a**) Organic carbon, (**b**) inorganic carbon).

Our analysis revealed that TN exerted the most substantial direct effect on SOC, with a path coefficient of 0.988, indicating its pivotal role in SOC accumulation. Previous studies [32] have highlighted that TN promotes plant growth, enhances root biomass, and stimulates microbial metabolic activity, thereby providing critical inputs to SOC while improving the stability of soil organic matter. Additionally, variables such as AI and SWC indirectly influence SOC by modulating soil moisture conditions. For instance, in arid and semi-arid regions, higher SWC facilitates greater vegetation cover and microbial activity, ultimately contributing to SOC storage [33]. Similarly, TP alleviates phosphorus limitations on plants and microbes, thereby enhancing SOC accumulation, particularly in nutrient-limited alpine regions [15]. Notably, soil pH exhibited a negative indirect effect on SOC, likely due to reduced microbial activity and inhibited organic matter decomposition in alkaline environments [34]. In contrast, the dynamics of SIC were primarily driven by the direct effects of geographical and climatic factors, particularly TEM, PET, and DEM. High PET intensifies evaporative processes, concentrating calcium and carbonate ions in the soil and facilitating carbonate precipitation [35]. DEM indirectly influences SIC by regulating TEM and PET; for instance, low temperatures and unique hydrological conditions in high-altitude regions may affect the dissolution and precipitation of carbonates. Moreover, an alkaline environment (pH > 8) significantly promotes carbonate formation, a critical factor in SIC accumulation. To optimize SIC fixation, specific land management practices, and climate change adaptation strategies can be employed. Adjusting irrigation regimes to balance PET can help reduce excessive evaporation, thus preventing the loss of water and promoting the conditions necessary for carbonate precipitation. By managing irrigation systems to ensure adequate water availability without excessive evaporation, we can regulate the soil moisture levels that influence both SOC and SIC. In addition, improving soil drainage conditions can mitigate the risk of waterlogging, which could otherwise reduce the efficiency of SIC accumulation by preventing carbonate precipitation. Furthermore, pH regulation through the use of soil amendments (e.g., adding lime or organic matter) can further enhance SIC sequestration, particularly in regions with more acidic soils. These land management practices, along with targeted adaptation measures to the unique climatic conditions of arid and semi-arid regions, could greatly improve the efficiency of SIC accumulation and make carbon sequestration more sustainable in the face of climate change.

These findings suggest that SOC dynamics are predominantly governed by soil physicochemical factors, whereas SIC dynamics are heavily dependent on geographical and climatic factors. This conclusion aligns with the environmental characteristics of high-altitude arid regions such as the Qinghai–Tibet Plateau and Qilian Mountains. In these areas, low temperatures and nutrient limitations contribute to SOC stability, while arid conditions create favorable environments for SIC precipitation. From a practical perspective, these results hold significant implications for regional soil management. For example, sustainable irrigation practices that enhance SWC can improve SOC storage, while regulating PET and pH may optimize SIC sequestration.

4. Discussion

4.1. SOC and SIC Relationship

Our investigation revealed a significant positive correlation between SOC and SIC ($r = 0.55$, $p < 0.01$), emphasizing their interconnected roles in the soil carbon cycle. SIC content increased with soil depth within the topsoil layer (<50 cm); however, beyond this critical depth, SIC declined with increasing soil depth. This finding partially contrasts with other studies, such as Zhang et al. [4] and Du et al. [21], which reported a consistent increase in SIC with soil depth due to carbonate precipitation in deeper soils. However, our results align with findings from regions such as the middle and lower Yellow River Delta [36], the North China Plain [22], and the Yanqi Basin in northwest China [23].

$$CO_2 + H_2O \rightleftharpoons HCO_3^- + H^+ \tag{1}$$

$$Ca^{2+} + 2HCO_3^- \rightleftharpoons CaCO_3 + CO_2 + H_2O \tag{2}$$

The positive SOC-SIC correlation can be explained through interactions mediated by CO_2 flux. SOC decomposition generates CO_2, which reacts with water to form HCO_3^- and H^+ (Equation (1)). HCO_3^- acts as a substrate for carbonate precipitation (Equation (2)), linking SOC and SIC formation. However, this relationship is influenced by environmental factors such as pH and water availability. For instance, higher H^+ concentrations in SOC-enriched regions may shift Equation (2) leftward, inhibiting carbonate formation. Conversely, under alkaline conditions, HCO_3^- promotes SIC accumulation [2,22].

In alpine regions, low temperatures and limited water movement in frozen soils reduce microbial activity and restrict carbonate dynamics. These constraints explain the diminished SIC accumulation beyond 50 cm in our study, contrasting with findings in temperate or subtropical zones [15]. The accumulation of SIC in the 10–50 cm layer reflects optimal conditions for carbonate precipitation, including moderate water availability and favorable pH [12,35]. At greater depths, lower temperatures and reduced CO_2 flux suppress SIC formation, highlighting the importance of environmental constraints in shaping SOC-SIC dynamics. Our findings underscore the complementary roles of SOC and SIC in soil carbon storage. SOC serves as a dynamic carbon pool concentrated in surface soils, while SIC represents a more stable reservoir in subsoil layers. The interaction between these pools in alpine ecosystems is modulated by freeze–thaw cycles, hydrological processes, and pH gradients. These dynamics are crucial for understanding carbon storage in regions affected by permafrost and seasonal freeze–thaw cycles.

The positive correlation between SOC and SIC observed in our study is not unique to alpine ecosystems. Across different ecosystems globally, this relationship appears to hold, with variations depending on local environmental factors such as temperature, precipitation, soil type, and vegetation cover. For instance, studies in temperate regions and tropical forests have similarly observed a positive correlation between these two carbon pools [22,23,36], though the relative contribution of each may vary. In arid and semi-arid regions, however, SIC can sometimes dominate, especially in regions where carbonate precipitation is favored by the climate [4,21]. As global changes, particularly climate change and land use change, continue to impact ecosystems, the relationship between SOC and SIC may evolve. Climate change may alter precipitation patterns, increase temperatures, and affect the freeze–thaw cycles in colder regions, all of which could influence the rates of both SOC decomposition and SIC formation. In arid regions, for example, increased temperatures and altered precipitation regimes could promote more rapid carbonate precipitation, increasing SIC formation. On the other hand, changes in land use, such as agricultural expansion or deforestation, could modify the input of organic matter to the soil, which would affect SOC dynamics and potentially disrupt the balance between SOC and SIC.

From a global perspective, understanding how SOC and SIC interact under changing climatic and land use conditions is critical for predicting future soil carbon dynamics. Further research is needed to assess how these relationships may change under different climate scenarios, particularly in regions experiencing rapid environmental shifts.

This study demonstrates that SOC and SIC not only differ significantly in spatial distribution but also contribute distinctively to carbon storage. SOC is primarily concentrated in the surface layer (0–30 cm), accounting for 81.62% of the total soil carbon, while SIC is predominantly found between 50 and 70 cm and continues to accumulate in deeper soil layers. This aligns with the findings of Wang et al. [12], which suggest that, in arid and cold environments, SIC serves as a long-term stable carbon pool, whereas SOC is more influenced by biological processes and its storage fluctuates with environmental conditions. Moreover, SOC is affected by vegetation productivity and microbial degradation, whereas SIC is more regulated by carbonate chemical processes [15]. In high-altitude ecosystems, SOC accumulation is limited by temperature, precipitation, and vegetation type, while SIC deposition is influenced by evaporation and the availability of Ca^{2+}. Consequently, in regional carbon balance, SOC provides a rapid cycling source of active carbon, while SIC functions as a long-term, stable carbon reservoir.

4.2. Controlling the Drivers of SOC Change

Soil nutrients, particularly TN and TP, are widely acknowledged as pivotal drivers of SOC dynamics (Figure 6). TN enhances soil nitrogen availability, supporting plant growth and increasing litter inputs to SOC pools [37]. TP alleviates phosphorus limitation in high-altitude regions, further promoting vegetation productivity and organic matter input to soils [15]. Beyond nutrient inputs, environmental factors such as SWC and AI significantly influence SOC. Higher SWC and humid conditions enhance vegetation growth and SOC input, but they may also create anaerobic conditions, inhibiting SOC decomposition [38]. Soil pH is another key factor influencing SOC dynamics. Low pH constrains microbial diversity and activity, reducing organic matter decomposition and promoting SOC accumulation. In contrast, a high pH restricts vegetation nutrient uptake by sequestering essential elements like nitrogen and iron in the soil matrix [18]. Correlation analyses further revealed that silt-rich soils support higher SOC stocks than gravelly soils due to their superior adsorption and water retention properties [34].

Elevation indirectly impacts SOC dynamics by modulating temperature and vegetation productivity. In our study, elevations exceeding 3600 m were characterized by low temperatures that constrained vegetation growth and reduced litter inputs, limiting SOC accumulation [33,39]. However, the 3300–3600 m range emerged as a SOC hotspot, likely due to optimal temperature and water availability that promote vegetation productivity. Future climate change may pose a risk to this carbon-rich zone, as warming temperatures could accelerate SOC decomposition and result in significant carbon losses.

The storage capacity of SOC is influenced not only by nutrients (such as TN and TP) but also by soil texture and land use type. In the study area, SOC is primarily concentrated in the surface layer (0–30 cm), while deeper SOC accumulation is relatively low, which may be related to low temperatures and limited microbial activity [22]. Moreover, SOC content shows significant variation across different land use types (Table 1). In grassland systems, SOC content is higher (49.65 g kg^{-1}, 0–10 cm), while shrubland systems exhibit even higher SOC content (69.6 g kg^{-1}, 0–10 cm), which may be attributed to differences in plant biomass and litter input [34]. These results suggest that grassland and shrubland ecosystems play a vital role in soil carbon sequestration, especially in arid and semi-arid regions. Another important aspect of SOC storage is its stability. Although SOC is a key component of the soil carbon pool, it is highly susceptible to microbial decomposition and climate change. Under rising temperatures, SOC may decompose more rapidly due to enhanced microbial activity, leading to carbon release.

4.3. Controlling the Drivers of SIC Change

Our study revealed that SIC levels in the HRB exhibited a relatively low profile, markedly distinct from semi-arid regions of northwest China [4] and closely akin to findings from the hinterlands of the QTP [21]. This discrepancy reflects the contrasting effects of regional water availability, evaporation, and temperature gradients. In the HRB, a negative correlation between SIC, SWC, and AI suggests that arid conditions favor SIC accumulation, a trend supported by numerous studies [12,40–42].

$$CaCO_3 + 2H^+ \rightleftharpoons Ca^{2+} + H^+ + HCO_3^- \rightleftharpoons Ca^{2+} + CO_2 + H_2O \quad (3)$$

The influence of elevation on SIC dynamics is typically mediated by environmental factors such as temperature and evaporation. In general, as the elevation increases, the temperature decreases, which attenuates the SOC decomposition rates and subsequently reduces CO_2 emissions (Section 4.1). Simultaneously, increased evaporation rates contribute to substantial SIC accumulation within the soil [18]. Furthermore, lower soil pH levels, which typically signify elevated concentrations of H^+ ions in the soil, prompt Equation (3) to shift toward reduced carbonate production [38]. The impact of TK on SIC dynamics is predominantly indirect, primarily exerted through its influence on plant growth and the regulation of soil pH levels [17].

The storage capacity of SIC plays a crucial role in the carbon cycle. Compared to SOC, SIC forms at a slower rate but exhibits much higher stability, allowing it to persist in the soil for thousands of years [36]. In the study area, SIC storage peaks at a depth of 50–70 cm and gradually decreases in deeper layers. This pattern suggests that SIC has a high accumulation potential in mid-depth soils, particularly in arid regions where carbonate precipitation conditions are favorable [38]. Due to its long-term stability, the role of SIC in regional carbon balance cannot be overlooked. Recent studies have shown that

SIC may provide a long-term buffering effect on CO_2 through dissolution–precipitation processes [4]. Therefore, although SIC exhibits low short-term dynamics, its contribution to long-term carbon sequestration warrants attention in global carbon management strategies. Future research should further quantify SIC storage rates and assess its dynamic changes under different land use practices.

4.4. Implication for Carbon Management

Although situated in an arid region, the HRB predominantly relies on SOC as the primary source of its soil carbon pool. This finding deviates from those of studies conducted in arid regions [2,4,15]. However, this pattern is consistent with the observations in the northern QTP, as evidenced by Du and Gao [21]. We propose that this discrepancy stems from the inhibitory effects of the cold climate of the region on SIC accumulation. Reports from the second Chinese scientific expedition to the QTP indicate an unprecedented process of warming and humidification, which is particularly pronounced in mountainous areas, such as the HRB [43]. This climatic shift has multifaceted implications for carbon dynamics. Warming temperatures increase soil temperatures and promote microbial activity and soil respiration in alpine mountain ecosystems, which can lead to carbon pool loss. Conversely, climate warming extends the accumulated temperature, thereby prolonging the growing season, enhancing vegetation productivity, and increasing the source of soil carbon input. Furthermore, climate warming accelerates glacial melting, extends vegetation growth limits, and augments the soil carbon pool. Melting glacial water also promotes vegetation growth. However, the relatively minimal carbon stored in deep permafrost (Sections 3.1 and 3.2) mitigates the release of significant carbon volumes upon permafrost thawing.

Although the current impact of climate warming on soil carbon loss in the HRB may not be readily apparent, it is crucial to acknowledge its potential consequences, particularly given the high SOC levels observed within the elevation range of 3300–3600 m. Any damage to the alpine soil carbon pool could have irreversible effects on the economy and society of the region. The predominance of SOC in the soil carbon pool suggests that nutrient management practices should prioritize enhancing SOC sequestration. Conversely, managing SIC requires mitigating abiotic stressors such as potential evapotranspiration and temperature. These findings provide actionable insights for policymakers and land managers aiming to optimize carbon storage in arid alpine regions. First, stringent ecological protection measures must be upheld, accompanied by active efforts to restore grasslands degraded by human activity and other factors. In addition, expanding low-shrub planting could be considered to mitigate rising surface temperatures, thereby reducing the rate of soil carbon release brought about by increased microbial activity. However, it is important to recognize that ecological restoration and the expansion of low-shrub planting will inevitably increase ecological water demand. This increased demand could potentially lead to a reduction in runoff production capacity, exacerbating the imbalance between the water resource supply and demand. These factors highlight the need for careful consideration and strategic planning for future ecological protection and resource management.

5. Conclusions

In this study, we investigated the soil profile from the surface to the bedrock in the Heihe River Basin (HRB) of the northeastern Qinghai–Tibet Plateau (QTP), China, to analyze the distribution patterns of soil organic carbon (SOC) and soil inorganic carbon (SIC), quantifying the influence of various environmental factors and elucidating the primary influencing pathways. The main conclusions are as follows:

1. In the arid alpine ecosystem of the HRB, SOC, and SIC exhibit distinct spatial and vertical distribution patterns. SOC increases with elevation, peaking at 42.96 ± 4.86 g/kg

within the 3300–3600 m range, before declining at higher elevations. In contrast, SIC decreases continuously with elevation, reflecting the influence of abiotic factors such as temperature, evaporation, and water dynamics, while SOC is primarily driven by biological processes like vegetation productivity and organic matter inputs. SOC is concentrated in surface soils, whereas SIC accumulation is most pronounced in the 10–50 cm soil layer, shaped by hydrological and chemical constraints on carbonate formation.

2. A significant positive correlation between SOC and SIC (r = 0.55, $p < 0.01$) highlights their interconnected roles in the soil carbon cycle. SOC decomposition generates CO2, which facilitates carbonate formation. However, higher elevations with lower temperatures and freeze–thaw cycles limit this process, particularly in deeper soil layers (>50 cm), where SIC accumulation declines. These findings underscore the dynamic coupling of SOC and SIC, regulated by both biological and abiotic factors. This coupling should be considered when designing carbon management strategies that balance the conservation of both organic and inorganic carbon pools.
3. SOCD constitutes 81.62% of the total soil carbon pool, dominating carbon storage in the HRB. However, SOC-rich zones (3300–3600 m) are vulnerable to warming-induced carbon release, threatening the stability of the regional carbon pool. To mitigate these risks and preserve soil carbon storage, we propose the following region-specific carbon management strategies:
   (a). Vegetation Conservation: Prioritize the restoration and expansion of vegetation, particularly in SOC-rich areas, to enhance carbon input.
   (b). Water and pH Management: Optimize water resource management to support vegetation growth and SOC accumulation while adjusting the soil pH to promote SIC formation.
   (c). Climate Adaptation: Implement measures to mitigate warming impacts on permafrost and soil carbon pools, such as reducing surface disturbance and enhancing vegetation cover.

These strategies are essential in preserving soil carbon pools in arid alpine regions and supporting long-term carbon sequestration under changing climatic conditions.

Author Contributions: Conceptualization, M.Z. and G.C.; data curation, Q.Z.; investigation, Q.H. and X.Q.; methodology, M.Z.; project administration, G.C.; resources, F.Z. and H.L.; software, M.Z.; supervision, Y.M.; validation, G.C.; writing—original draft, M.Z.; writing—review and editing, M.Z. and G.C. All authors have read and agreed to the published version of the manuscript.

Funding: Natural Science Foundation of the Qinghai Province (grant no. 2023-ZJ-907M).

Data Availability Statement: Dataset available on request from the authors.

Conflicts of Interest: The authors declare no known conflicts of interest.

References

1. Prommer, J.; Walker, T.W.N.; Wanek, W.; Braun, J.; Zezula, D.; Hu, Y.; Hofhansl, F.; Richter, A. Increased microbial growth, biomass, and turnover drive soil organic carbon accumulation at higher plant diversity. *Glob. Chang. Biol.* **2020**, *26*, 669–681. [CrossRef] [PubMed]
2. Sharififar, A.; Minasny, B.; Arrouays, D.; Boulonne, L.; Chevallier, T.; Van Deventer, P.; Field, D.J.; Gomez, C.; Jang, H.-J.; Jeon, S.-H.; et al. Soil inorganic carbon, the other and equally important soil carbon pool: Distribution, controlling factors, and the impact of climate change. In *Advances in Agronomy*; Elsevier: Amsterdam, The Netherlands, 2023; pp. 165–231.
3. Batjes, N.H. Total carbon and nitrogen in the soils of the world. *Eur. J. Soil Sci.* **2014**, *65*, 10–21. [CrossRef]
4. Zhang, F.; Wang, X.; Guo, T.; Zhang, P.; Wang, J. Soil organic and inorganic carbon in the loess profiles of Lanzhou area: Implications of deep soils. *CATENA* **2015**, *126*, 68–74. [CrossRef]
5. Li, Z.; Han, F.; Su, Y.; Zhang, T.; Sun, B.; Monts, D.; Plodinec, M. Assessment of soil organic and carbonate carbon storage in China. *Geoderma* **2007**, *138*, 119–126. [CrossRef]

6. Wu, H.; Guo, Z.; Gao, Q.; Peng, C. Distribution of soil inorganic carbon storage and its changes due to agricultural land use activity in China. *Agric. Ecosyst. Environ.* **2009**, *129*, 413–421. [CrossRef]
7. Lal, R. Soil Carbon Sequestration Impacts on Global Climate Change and Food Security. *Science* **2004**, *304*, 1623–1627. [CrossRef]
8. Chen, F.; Feng, P.; Harrison, M.T.; Wang, B.; Liu, K.; Zhang, C.; Hu, K. Cropland carbon stocks driven by soil characteristics, rainfall and elevation. *Sci. Total Environ.* **2023**, *862*, 160602. [CrossRef]
9. Choudhury, B.U. Controls on vertical distribution of organic carbon in the intermontane valley soils (Barak, Northeast India). *Soil Tillage Res.* **2023**, *225*, 105532. [CrossRef]
10. Niu, S.; Song, L.; Wang, J.; Luo, Y.; Yu, G. Dynamic carbon-nitrogen coupling under global change. *Sci. China Life Sci.* **2023**, *66*, 771–782. [CrossRef]
11. Le, C.; Andrew, R.M.; Friedlingstein, P.; Sitch, S.; Hauck, J.; Pongratz, J.; Pickers, P.A.; Korsbakken, J.I.; Peters, G.P.; Canadell, J.G.; et al. Global Carbon Budget 2018. *Earth Syst. Sci. Data* **2023**, *10*, 2141–2194.
12. Wang, S.; Zhuang, Q.; Zhou, M.; Jin, X.; Yu, N.; Yuan, T. Temporal and spatial changes in soil organic carbon and soil inorganic carbon stocks in the semi-arid area of northeast China. *Ecol. Indic.* **2023**, *146*, 109776. [CrossRef]
13. Plaza, C.; Zaccone, C.; Sawicka, K.; Méndez, A.M.; Tarquis, A.; Gascó, G.; Heuvelink, G.B.M.; Schuur, E.A.G.; Maestre, F.T. Soil resources and element stocks in drylands to face global issues. *Sci. Rep.* **2018**, *8*, 13788. [CrossRef] [PubMed]
14. Lal, R. Carbon Cycling in Global Drylands. *Curr. Clim. Chang. Rep.* **2019**, *5*, 221–232. [CrossRef]
15. Ren, Z.; Li, C.; Fu, B.; Wang, S.; Stringer, L.C. Effects of aridification on soil total carbon pools in China's drylands. *Glob. Chang. Biol.* **2024**, *30*, e17091. [CrossRef]
16. Rawlins, B.; Henrys, P.; Breward, N.; Robinson, D.; Keith, A.; Garcia-Bajo, M. The importance of inorganic carbon in soil carbon databases and stock estimates: A case study from England. *Soil Use Manag.* **2011**, *27*, 312–320. [CrossRef]
17. Tao, J.; Raza, S.; Zhao, M.; Cui, J.; Wang, P.; Sui, Y.; Zamanian, K.; Kuzyakov, Y.; Xu, M.; Chen, Z.; et al. Vulnerability and driving factors of soil inorganic carbon stocks in Chinese croplands. *Sci. Total Environ.* **2022**, *825*, 154087. [CrossRef]
18. Liu, X.; Lu, X.; Yu, R.; Sun, H.; Li, X.; Li, X.; Qi, Z.; Liu, T.; Lu, C. Distribution and storage of soil organic and inorganic carbon in steppe riparian wetlands under human activity pressure. *Ecol. Indic.* **2022**, *139*, 108945. [CrossRef]
19. Wang, Z.; Han, X.; Chang, S.; Wang, B.; Yu, Q.; Hou, L.; Li, L. Soil organic and inorganic carbon contents under various land uses across a transect of continental steppes in Inner Mongolia. *CATENA* **2013**, *109*, 110–117. [CrossRef]
20. Han, X.; Gao, G.; Chang, R.; Li, Z.; Ma, Y.; Wang, S.; Wang, C.; Lü, Y.; Fu, B. Changes in soil organic and inorganic carbon stocks in deep profiles following cropland abandonment along a precipitation gradient across the Loess Plateau of China. *Agric. Ecosyst. Environ.* **2018**, *258*, 1–13. [CrossRef]
21. Du, C.; Gao, Y. Opposite patterns of soil organic and inorganic carbon along a climate gradient in the alpine steppe of northern Tibetan Plateau. *CATENA* **2020**, *186*, 104366. [CrossRef]
22. Shi, H.; Wang, X.; Zhao, Y.; Xu, M.; Li, D.; Guo, Y. Relationship between soil inorganic carbon and organic carbon in the wheat-maize cropland of the North China Plain. *Plant Soil* **2017**, *418*, 423–436. [CrossRef]
23. Wang, X.; Wang, J.; Xu, M.; Zhang, W.; Fan, T.; Zhang, J. Carbon accumulation in arid croplands of northwest China: Pedogenic carbonate exceeding organic carbon. *Sci. Rep.* **2015**, *5*, 11439. [CrossRef] [PubMed]
24. Mi, N.; Wang, S.; Liu, J.; Yu, G.; Zhang, W.; Jobbágy, E. Soil inorganic carbon storage pattern in China. *Glob. Chang. Biol.* **2008**, *14*, 2380–2387. [CrossRef]
25. Bachman, G.O.; Machette, M.N. *Calcic Soils and Calcretes in the Southwestern United States*; (No. 77-794); United States Department of the Interior Geological Survey: Reston, VA, USA, 1977.
26. Li, Z.; Li, W.; Li, Z.; Lv, X. Responses of Runoff and Its Extremes to Climate Change in the Upper Catchment of the Heihe River Basin, China. *Atmosphere* **2023**, *14*, 539. [CrossRef]
27. Han, P.; Huang, C.; Liang, S.; Feng, Y.; Wan, L. Variation characteristics and quantitative study of permafrost degradation in the upper reaches of Heihe River, China. *J. Hydrol.* **2022**, *610*, 127942. [CrossRef]
28. Walter, K.; Don, A.; Tiemeyer, B.; Freibauer, A. Determining Soil Bulk Density for Carbon Stock Calculations: A Systematic Method Comparison. *Soil Sci. Soc. Am. J.* **2016**, *80*, 579–591. [CrossRef]
29. Dai, L.; Ge, J.; Wang, L.; Zhang, Q.; Liang, T.; Bolan, N.; Lischeid, G.; Rinklebe, J. Influence of soil properties, topography, and land cover on soil organic carbon and total nitrogen concentration: A case study in Qinghai-Tibet plateau based on random forest regression and structural equation modeling. *Sci. Total Environ.* **2022**, *821*, 153440. [CrossRef]
30. Yang, Y.; Fang, J.; Tang, Y.; Ji, C.; Zheng, C.; He, J.; Zhu, B. Storage, patterns and controls of soil organic carbon in the Tibetan grasslands: Soil organic carbon in Tibetan grasslands. *Glob. Chang. Biol.* **2008**, *14*, 1592–1599. [CrossRef]
31. Zhang, X.; Li, X.; Ji, X.; Zhang, Z.; Zhang, H.; Zha, T.; Jiang, L. Elevation and total nitrogen are the critical factors that control the spatial distribution of soil organic carbon content in the shrubland on the Bashang Plateau, China. *CATENA* **2021**, *204*, 105415. [CrossRef]
32. Wu, G.; Huang, G.; Lin, S.; Huang, Z.; Cheng, H.; Su, Y. Changes in soil organic carbon stocks and its physical fractions along an elevation in a subtropical mountain forest. *J. Environ. Manag.* **2024**, *351*, 119823. [CrossRef]

33. Zhu, M.; Feng, Q.; Zhang, M.; Liu, W.; Qin, Y.; Deo, R.C.; Zhang, C. Effects of topography on soil organic carbon stocks in grasslands of a semiarid alpine region, northwestern China. *J. Soils Sediments* **2019**, *19*, 1640–1650. [CrossRef]
34. Zhang, H.; Yin, A.; Yang, X.; Wu, P.; Fan, M.; Wu, J.; Zhang, M.; Gao, C. Changes in surface soil organic/inorganic carbon concentrations and their driving forces in reclaimed coastal tidal flats. *Geoderma* **2019**, *352*, 150–159. [CrossRef]
35. Stanbery, C.; Ghahremani, Z.; Huber, D.; Will, R.; Benner, S.; Glenn, N.; Hanif, T.; Spaete, L.; Terhaar, D.; Lohse, K.A.; et al. Controls on the presence and storage of soil inorganic carbon in a semi-arid watershed. *CATENA* **2023**, *225*, 106980. [CrossRef]
36. Guo, Y.; Wang, X.; Li, X.; Xu, M.; Li, Y.; Zheng, H.; Luo, Y.; Smith, P. Impacts of land use and salinization on soil inorganic and organic carbon in the middle-lower Yellow River Delta. *Pedosphere* **2021**, *31*, 839–848. [CrossRef]
37. Ma, Y.; Xie, T.; Li, X. Spatial variation of soil organic carbon in the Qinghai Lake watershed, northeast Qinghai-Tibet Plateau. *CATENA* **2022**, *213*, 106187. [CrossRef]
38. Zhao, W.; Zhang, R.; Cao, H.; Tan, W. Factor contribution to soil organic and inorganic carbon accumulation in the Loess Plateau: Structural equation modeling. *Geoderma* **2019**, *352*, 116–125. [CrossRef]
39. Chen, L.; He, Z.; Du, J.; Yang, J.; Zhu, X. Patterns and environmental controls of soil organic carbon and total nitrogen in alpine ecosystems of northwestern China. *CATENA* **2016**, *137*, 37–43. [CrossRef]
40. Hussain, S.; Sharma, V.; Arya, V.M.; Sharma, K.R.; Rao, C.S. Total organic and inorganic carbon in soils under different land use/land cover systems in the foothill Himalayas. *CATENA* **2019**, *182*, 104104. [CrossRef]
41. You, M.; Han, X.; Hu, N.; Du, S.; Doane, T.A.; Li, L. Profile storage and vertical distribution (0–150 cm) of soil inorganic carbon in croplands in northeast China. *CATENA* **2020**, *185*, 104302. [CrossRef]
42. Pfeiffer, M.; Padarian, J.; Vega, M.P. Soil inorganic carbon distribution, stocks and environmental thresholds along a major climatic gradient. *Geoderma* **2023**, *433*, 116449. [CrossRef]
43. Zhao, M.; Cao, G.; Cao, S.; Liu, F.; Yuan, J.; Zhang, Z.; Diao, E.; Fu, J. Spatial-temporal variation characteristics of land surface temperature in Qinghai Province from 1980 to 2017. *Arid Zone Res.* **2021**, *38*, 178–187.